Dalton Transactions

Accepted Manuscript

ROYAL SOCIETY OF CHEMISTRY

www.rsc.org/dalton

Theoretical Investigation of the Charge-Transfer Properties in Different Meso-linked Zinc Porphyrin for Highly Efficient Dye-Sensitized Solar Cells

Attempting to improve photoinduced intramolecular-charged transfer ability of meso-linked zinc porphyrin sensitizer, the strong withdrawing group (CN) was introduced into anchoring group. The strong charge-transfer character of new-designed dye dramatically increased.

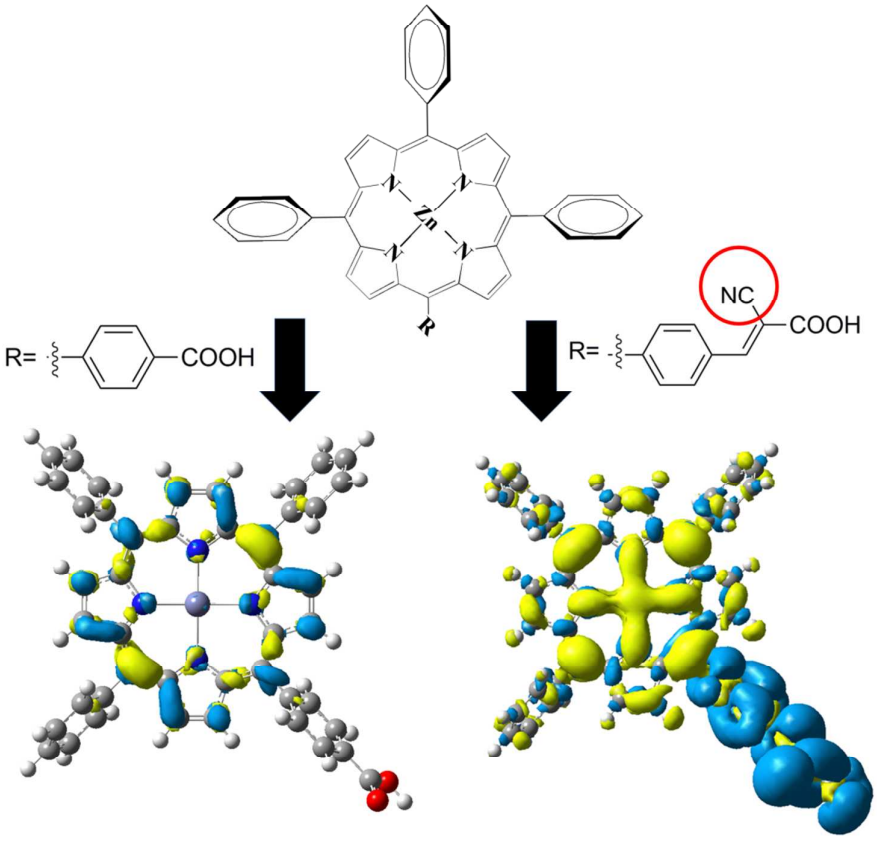

Theoretical Investigation of the Charge-Transfer Properties in Different Meso-linked Zinc Porphyrin for Highly Efficient Dye-Sensitized Solar Cells

Supawadee Namuangruk[1], Kanokkorn Sirithip[2], Rattanawelee Rattanatwan[3], Tinnagon Keawin[3], Nawee Kungwan[4], Taweesak Sudyodsuk[3], Vinich Promarak[5], Siriporn Jungsuttiwong[3,*]

[1]National Nanotechnology Center, National Science and Technology Development Agency, Klong Luang, Pathumthani 12120, Thailand

[2]Department of Science and Technology, Faculty of Arts and Sciences, Roi-Et Rajabhat University, Roi-Et, 45120, Thailand

[3]Center for Organic Electronic and Alternative Energy, Department of Chemistry and Center of Excellence for Innovation in Chemistry, Faculty of Science, Ubon Ratchathani University, Ubon Ratchathani 34190, Thailand

[4]Department of Chemistry, Faculty of Science, Chiang Mai University, Chiang Mai 50200, Thailand

[5]School of Chemistry and Center of Excellence for Innovation in the Chemistry, Institute of Science, Suranaree University of Technology, Nakhon Ratchasima 30000, Thailand

1. Introduction

Dye-sensitized solar cells (DSCs) have offered new opportunities in environmental friendliness and low-cost fabrication alternatives to the conventional silicon-based solar cell.[1, 2] The most successful sensitizers were firstly reported by Grätzel's group (1991) when considering the use of ruthenium complexes as sensitizers, promising the greatest performance for a solar-to-electric conversion efficiency of 10-11% under standard global air mass (AM) 1.5 solar conditions.[3-5] However, ruthenium dyes are very expensive due to the lack of abundance of natural ruthenium together with their undesirable environmental impact. Therefore, research is now directed toward finding cheaper and safer dyes, such as organic-based dyes or Ruthenium-free dyes.[6, 7] Among organic-based dyes, synthetic porphyrins have attracted much interest as light harvesters in DSCs due to their ability to modify and tune the photo-physical properties via optimizing the *β*- or *meso*-substituents of the porphyrin core.[8-12] The highest-performing porphyrin-based DSC sensitizer is a zinc porphyrin sensitizer, namely YD2-oC8, co-sensitized with an organic dye (Y123) on a TiO_2 film using a cobalt-based electrolyte to enhance photo-voltage of the device, which shows an overall conversion efficiency of 12.3% under standard AM 1.5 one-sun irradiation.[13] The UV/visible absorption spectra of porphyrin are of importance when designing them as sensitized for solar cells. The natural role in light harvesting is strong absorption in the range of 400-700 nm (400-450 nm: Soret (B)-band and 500-700 nm: Q-band.[14] This is caused by the splitting of the key frontier molecular orbitals (FMOs) of Gouterman's four orbital model ($HOMO_{-1}$, HOMO, LUMO, and $LUMO_{+1}$ orbitals)[15] which has been widely used when explaining the absorption spectra of porphyrins. According to this theory, the absorption bands in a porphyrin system arise from a transition between two HOMOs and two LUMOs. The HOMOs were calculated to be nearly degenerate the a_{1u} and a_{2u} orbitals while the LUMOs were calculated to be a degenerate set of the e_g orbitals (**Figure 1**a). Mixing splits these two states in energy by a

configuration interaction into two pairs of degenerate, creating a higher energy ^1E_u state with greater oscillator strength, giving rise to the Soret band, and a lower energy ^1E_u state with less oscillator strength, giving rise to the Q-band (**Figure 1**b). It is the identities of the metal center and the substituents on the ring that affect the relative energies of these transitions.

To develop a highly efficient porphyrin sensitizer for DSCs, a dye must be designed to have following properties: (i) the dye should absorb light in wide regions, particularly in the visible and near-IR regions to produce a large photocurrent response, (ii) it must contain attachment groups such as carboxylate or cyanoacrylate moieties to anchor the TiO_2 surface and inject electrons into the conduction band of TiO_2, (iii) the energy level of the highest occupied molecular orbital (HOMO) must be situated slightly above the conduction band of the TiO_2, and the lowest unoccupied molecular orbital (LUMO) must be located below the redox couple of the electrolyte solution such as I^-/I_3^-, (iv) the HOMO and LUMO should localize plentifully on the donor and acceptor of dye respectively, in order to process the efficient charge separation. According to DSCs requirements, the basic structure of a dye should comprise of an electron donor (D) (e.g. carbazole, triphenylamine, porphyrin, coumarin), a conjugated bridge (π) (e.g. benzene, thiophene, furan), and an electron acceptor (A) (e.g. carboxylic acid, cyanoacrylic acid) to form a D-π-A systems.[16-21] This system plays an important role in producing photo-induced intramolecular-charged transfer (ICT) property due to it being suitably tuned by matching the variety of appropriate groups.

In order to establish guidelines for the design of efficient DSC sensitizers, quantum chemical calculations were used to provide a useful theoretical basis for the geometric and electronic structure of sensitizer materials.[22-24] Walsh et al. reported the use of density functional theory (DFT) and time-dependent DFT (TDDFT) with B3LYP to predict a series of Zn-tetraphenylporphines with different conjugated functional groups at the *β*-position.[25] Ma et al. presented the use of DFT/TDDFT as a screening tool to predict the sensitizer

candidates of porphyrin analogues, which have 11 different kinds of substituted bridges.[26] Their results reveal that the candidates selected are very promising and provide good performances as sensitizers, challenging the current photoelectric conversion efficiency record of 7.1% of porphyrin-sensitized solar cells.[9] Recently, Balanay et al. predicted the trend in absorption spectra and photovoltaic properties using TD-CAM-B3LYP/6-31G(d)//B3LYP/6-31G(d) theoretical method.[27] These reveal that the computational calculations are capable for providing good performances, which show a promising outlook for computation-aided sensitizer design with anticipated good properties.

Previous results have shown that porphyrins ZnTCPP (TCPP = tetrakis(4-carboxyphenylporphine) have almost indistinguishable electron injection and recombination kinetics compared to ruthenium dye N3,[28] consequently they may eventually compete with devices based on Ru-complexes. Previous studies indicated that the π-conjugation in the β-substituted porphyrins has a limited effect of extending the absorption spectra to a greater wavelength.[29, 30] The best strategy to extend the π-conjugation is thus to functionalize the target porphyrin at the meso-positions.[31] Moreover, the close π-π aggregations of Porphyrins in solution lead to self-quenching and reduction of electron injection into TiO_2 that could decrease the efficiency of the sensitizer. This effect can be reduced by attaching bulky aryl substituent in the *meso*-position of the porphyrin core.[32]

Therefore, the goal of this present work is to investigate the effects of different *meso*-substituted linkages for **A1**, **B1**, and **C1** porphyrin analogues based on porphyrins ZnTCPP (as shown in **Figure 2**), with typical porphyrin moieties as donors and the carboxyl-containing groups as acceptors. Moreover, we designed a new dye-sensitizer by replacing acetic acid moiety with cyanoacrylic acid to improve the photoinduced intramolecular-charged transfer ability of meso-linked zinc porphyrin sensitizer, which is a challenging problem for processing the efficient charge separation to inject electrons effectively into the

conduction band of TiO_2 in the DSC devices. The geometry of our new-designed sensitizers, electronic structures and excited-state properties were reasonably investigated theoretically. Finally, the calculated results were compared with our experimental results[33] which will be published at a later date. The successful study of these theoretical calculations may be used as the first attempt to tune the molecular orbital energy levels and improve the light absorption properties in the screening step, providing new design effective sensitizers in further experimental synthesis.

2. Computational Details

The geometries and electronic structures of **A1**, **B1**, and **C1** porphyrin analogues were theoretical studied, based on Kohn-Sham density functional theory (DFT). Beck's three parameter gradient-corrected hybrid functional and Lee-Yang-Parr correlation functional (B3LYP)[34-36] with a 6-31G (d,p) basis set were used for full geometry optimization without any symmetry constrains. The natural bond orbital (NBO) was obtained using a POP=NBO keyword. The vertical excitation energies for the 20 lowest spin-allowed singlet transitions were investigated using time-dependent DFT (TDDFT)[37] on B3LYP hybrid functional. In order to increase more accuracy of TDDFT calculation, several Pople basis sets such as 6-31G(d,p), 6-311G(d,p), 6-31+G(d,p), and 6-311+G(d,p) were performed. The solvent effect as well as the electrostatic solute-solvent interactions in dichloromethane (CH_2Cl_2) solvent was evaluated using SCRF approach on conductor-like polarized continuum model (C-PCM) framework.[38] All DFT and TDDFT calculations were done using the Gaussian09 program package.[39] The UV/Vis absorption spectra were simulated using the SWizard program (Revision 4.6),[40] using the Gaussian model with the half-bandwidths ($\Delta_{1/2}$) which was taken to be equal to 3000 cm^{-1}. Density of state (DOS) analysis was calculated using the GausSum program.[41]

To gain insight into the electron injection capability of dyes, the adsorption of dyes on the $(TiO_2)_{38}$ cluster was performed with DFT calculations using the DMol^3 program[42, 43] in Materials Studio version 5.5. The structure of $(TiO_2)_{38}$ was comprised of 38 TiO_2 units, which modeled a TiO_2 nanoparticle, as in the researchers' previous report.[44] The $(TiO_2)_{38}$ configuration was fully optimized using the generalized gradient-corrected approximation (GGA) method. The Perdew-Burke-Ernzerhof (PBE)[45] functional was used to account exchange-correlation effects with DNP basis set. The core electron was treated with DFT-semicore Pseudopotentials (DSPPs).[43] The real space cut-off value was set to 5.0 Å, while the convergence criteria for optimization are 2.0 x 10^{-5} Ha, 4.0 x 10^{-3} Ha/Å, 5.0 x 10^{-3} Å for energy, gradient and atomic displacements, respectively. After optimization, the adsorption energy (E_{ads}) of dye on the $(TiO_2)_{38}$ cluster was obtained using the following equation:

$$E_{ads} = E_{dye} + E_{TiO2} - E_{dye+TiO2}$$

where E_{dye} is the total energy of isolated dye, E_{TiO2} is the total energy of $(TiO_2)_{38}$ cluster, and $E_{dye+TiO2}$ is the total energy of dye-$(TiO_2)_{38}$ complex. Following the above expression, the positive value of E_{ads} indicated a stable adsorption.

3. Results and Discussion

3.1 Geometric structure

The optimized geometries of **A1**, **B1**, and **C1** in their ground-state configurations by B3LYP/6-31G (d,p) are shown in **Figure 3**, and the selected bond lengths and dihedral angles parameters are listed in **Table 1**. The results show that the calculated Zn-N bond distances at the porphyrin core in all dyes were not significantly different. It should be noted that the addition of different π-conjugated molecules connected at the *meso*-position in porphyrin analogues slightly distorts the geometric structure of the porphyrin core, significant changes in geometrical parameters were found in dihedral angles (C4-C5-C25-C26). In order to extend conjugation length of π-spacer in **A1**, a benzene ring connected with a triple bond

were introduced, as in **B1.** We found that the dihedral angle between porphyrin and π-spacer were calculated to be 69.67 and 69.06 degrees for **A1** and **B1** respectively, which was slightly changed. Interestingly, replacement of the connected substituent of benzene ring by a thiophene unit in **C1** distinctly increase the dihedral angles to 75.52 degrees and therefore the geometric structure of **C1** was more twisted than that of **A1** and **B1,** the twisted angle are illustrated in the side view of ground-state optimized structure **(Figure 3)**. These findings imply that the delocalization of the π-electron from the porphyrin core to an acceptor group in **C1** cannot perform smoothly via the π-spacer linkage due to its twisted conformation and therefore, intramolecular charge transfer (ICT) should be decreased, the electron injection process could hardly occur. The more the conformation of the dyes were twisted, the lower the J_{SC} should be observed due to the J_{SC} value being related to the rate of electron injection to the photo-electrode, the more planar structure of **B1** showed significantly higher J_{SC} of 8.23 mA cm^{-2} than that of **C1** (7.14 mA cm^{-2}), see **Table2**. We found that the thiophene substituents played a lesser role in promoting the efficiency of DSSCs. We can therefore predict that the **B1** exhibits the best conversion efficiency, which is in excellent agreement with the best J_{SC} value of 8.23 mA cm^{-2} and a power conversion efficiency of 4.00% among our porphyrin dyes. Our results indicate that the different connected substituent groups at the *meso*-position of porphyrin directly affect the ground-state equilibrium structures, especially between the porphyrin macrocycle and the conjugated bridge.

3.2 NBO analysis and Electronic structures

To gain insight into the steric effect of a dye molecule, we employed the concept of the natural bond orbital (NBO) by analysis of the electronic atomic charge via B3LYP/ 6-31G(d,p) level of theory. The calculated NBO atomic charges are shown in **Figure 4**. However, as the charge of H atoms around the meso-position of **A1** and **B1** were similar, only **B1** will be discussed and compared with **C1**. The calculated atomic charges of H atoms

connected at C3 (H_{C3}) and C7 (H_{C7}) of the **B1**-porphyrin core were the same value (+0.150). In addition, the hydrogen atoms of the benzene-π-spacer connected to the meso-phorphyrin position (H_{C26} and H_{C30}) were calculated to be the same positive charge of +0.147. These hydrogen atoms interacting to each other, H_{C3} to H_{C26} and H_{C7} to H_{C30}, and resulted in hydrogen repulsion, therefore, these hydrogen atoms try to avoid each other providing a twisted dihedral angle between the porphyrin core and the π-bridge of about -69.06 degrees. For **C1**, the atomic charges, H_{C26} and S29, in the substituted thiophene ring were calculated to be +0.152 and +0.293, respectively. Obviously, the **C1**, with a greater positive charge on H atoms around the meso-position, performs two strongly repulsive forces between H_{C3} to H_{C26} and H_{C7} to S29. These mainly causes a more twisted dihedral angle of about 75.52 degrees. This discrepancy shows that the substitution of thiophene ring at the *meso*-position of a porphyrin core in **C1** can be a major cause of the largest dihedral angles between the porphyrin core and the π-bridge compared with **A1** and **B1**. Our NBO analysis implies that the substitution of the benzene ring by a thiophene unit in our system will increase the steric hindrance, leading to a greater twist conformation from the repulsion of atomic charges and will therefore resist charge transport from a porphyrin macrocycle and the *meso*-substituted linkages.

It is very useful to determine the highest occupied molecular orbital (HOMO) and the lowest unoccupied molecular orbital (LUMO) contribution of these analogues, as these can provide a reasonable qualitative indication of the charge-separated state of sensitizers. This can be rationalized by analysis of the electronic molecular orbital, where the HOMO must be primarily dominated by the HOMO of the donor, while the LUMO must be plentifully distributed on the acceptor moieties. The frontier molecular orbital plots of **A1**, **B1**, and **C1** by B3LYP/6-31G(d,p) are shown in **Figure 5**. In general, the HOMO possesses an antibonding character between the subunits, and the LUMO normally shows a bonding

character between the subunits. There were delocalized π orbitals dominantly located on the porphyrin core in HOMO, for all dyes. In LUMO, it was found that delocalization of electrons were mainly spread over the porphyrin core and partly spread on substituent linkages. Our calculations indicated that the ICT character took place only slightly. These results could be the main reason for our A1, B1 and C1 dye to perform relatively low power conversion efficiencies of 1.80, 4.00 and 3.24%, respectively compared to N3 reference-dye (7.87%), see Table 2. The ICT character improves the injection efficiency and thereby improves the photocurrents which mean the J_{SC} value being related to ICT character, our A1, B1 and C1 performed only small ICT character yielding small J_{SC} value of 3.96, 8.23 and 7.14 mA cm^{-2}, respectively compared to N3 (15.92 mA cm^{-2}). These results imply that it is possibly to further improve the efficiency of energy conversion via tuning photo-induced intramolecular-charged transfer ability of meso-linked zinc porphyrin sensitizer, we designed a new dye-sensitizer by replacing acetic acid moiety (in **A1**, **B1** and **C1**) as cyanoacrylic acid forming **A2**, **B2** and **C2** as shown in **Figure 6.**

When adding strong withdrawing group (CN), the density difference plot for the first lowest excitation (ρ_{S1}-ρ_{S0}) of **A2**, **B2** and **C2** exhibited a dramatically stronger ICT character compared to the dye without CN (**A1**, **B1** and **C1**), see **Figure 7**. Yellow and blue colours symbolize the decreased and increased electron contributions of the lowest energy excitation. **Figure 7** shows that adding electron-withdrawing groups increases the push-pull driving force. The electron contributions were pulled by anchoring group forming push-pull zinc porphyrin. Therefore, the withdrawing groups effectively enhanced charge separation and potentially increase the efficiency of electron injection and retarded charge recombination.

3.3 The molecular orbital energy

The HOMO-LUMO gaps of these analogues were computed using B3LYP/ 6-31G(d,p) level of theory in both vacuum and CH_2Cl_2 solvent. The calculated HOMO-

LUMO gaps and molecular orbital diagram are shown in **Table 2** and **Figure 8**. The calculated HOMO-LUMO gaps of **A1**, **B1**, and **C1** were 2.85, 2.82, and 2.84 eV, respectively. The results showed that extending the π-conjugated system by either adding ethylnylene-phenylene or ethylnylene-thiophene moieties can slightly decrease the HOMO-LUMO gap. The trend of band gap was in sequence of **B1** (2.82 eV) < **C1** (2.84 eV) < **A1** (2.85 eV), which was in close agreement with the experiment trend: **B1** (1.97 eV) < **C1** (1.98 eV) < **A1** (2.04 eV). Furthermore, our calculated band gap corresponds to our experimental photon-to-current conversion efficiency[33] of **B1** (4.00%) > **C1** (3.24%) > **A1** (1.80%) referenced by **N3** (7.87%), see **Table 2**. Distinctly, the smaller HOMO-LUMO gaps appeared to have the higher efficiency of the corresponding solar cell. This trend was supported by the theoretical prediction of Ma et al.[46] which anticipated that the lower energy gap of ZnTPPG (2.194 eV) is very promising as a challenge to the best conversion efficiency record of 7.1% in 2010 of the ZnTMPPI (2.298 eV) without co-sensitizer. The efficiencies of Zinc-porphyrin sensitized solar cells raise rapidly in the past few years, in 2011 the YD2-oC8, co-sensitized with an organic dye (Y123) shows the highest overall conversion efficiency of 12.3%.[13] Therefore we have been attempting to find out the relationship between the molecular and electronic structures of porphyrin sensitizers and the performances of the porphyrin-sensitizer. We found that our newly designed dyes (**A2**, **B2** and **C2**) can effectively decrease the energy gap, see **Figure 8.**

To study the abilities of the injection of an electron into the conduction band (CB) of a metal oxide particle and the regeneration reaction of an electron to the excited dyes, the molecular orbital energies will be analyzed. **Figure 8** shows the molecular orbital energy diagram for **A1**, **B1**, **C1**, **A2**, **B2** and **C2** by DFT calculation. In our previous report,[47] the HOMO, LUMO, HOMO-LUMO gap of $(TiO_2)_{38}$ in a stoichiometric anatase (101) surface using the PBE functional together with the DFT-semicore Pseudopotnetials (DSSPPS) were

calculated to be -7.972, -3.523, and 4.449 eV, respectively, while the lowest transition was reduced to 3.75 eV, which was reasonable higher than typical band gaps of TiO_2 nanoparticles.[48-51] As mention above, for a high-efficiency sensitizer of DSCs, the LUMO energies of dyes must be placed slightly above the conduction band of TiO_2 and the HOMO energies of dyes must be properly located under the redox couple of I^-/I_3^- electrolyte. From the results, it was found that the HOMO energies of all analogues were located lower than the redox couple of I^-/I_3^-, and LUMO laid above CB of TiO_2 as expected, the energy gap of all dyes were computed to be 2.82, 2.80 and 2.81 for **A1**, **B1** and **C1**, respectively and significantly lowering to 2.52, 2.35 and 2.41 for **A2**, **B2** and **C2**, respectively. These can be described as the adding of a strong withdrawing group efficiently improves the conjugated system in a dye sensitizer. Therefore, we successfully designed a new dye with a strong withdrawing group (**A2**, **B2** and **C2**) to potentially be a high efficient porphyrin-dye sensitized solar cell, especially the **B2**, which exhibited the lowest energy gap of 2.35 eV.

3.4 Excitation energies and UV/Vis absorption spectra

In order to understand the electronic transition, TDDFT calculations on excitation energies and UV/Vis absorption spectra for all dyes were performed. The 20 lowest singlet-singlet transitions, up to an energy of ~4.96 eV (250 nm), were investigated with B3LYP functional. To obtain more reliability, various basis sets such as 6-31G(d,p), 6-311G(d,p), 6-31+G(d,p), and 6-311+G(d,p) have been tested. The appropriate basis set was identified by predicted absorption spectra of all dyes from their ground-state optimized structures in CH_2Cl_2 solvent. The absorption spectra on several basis sets of **A1**, **B1** and **C1** are depicted in **Figure S1**. As shown in **Figure S1**, it was found that the predicted absorption spectra by 6-311+G(d,p) basis set for all analogues were red-shifted compared with 6-31+G(d,p), 6-311G(d,p), and 6-31G(d,p), respectively, which was closest to the experimental observation. In order that the detailed electronic microscopic information could be analyzed, only a 6-

311+G(d,p) basis set was used. The calculated excitation energies, oscillator strengths, and electronic configuration for all dyes using TD-B3LYP/6-311+G(d,p) level of theory are collated in **Table 3**.

The excitation energies and absorption spectra of these analogues have been analyzed and interpreted by considering the Gouterman's four-orbital model,[52] which is the intrinsic character of a porphyrin base. This model involves the transition of HOMO-1, HOMO, LUMO, and LUMO-1 orbitals, which cause the intense B- and weak Q-bands. From **Table 3**, it was found that the electronic excitation from HOMO to LUMO for all analogues can be considered as a mixed transition between charge transfer (CT) and π-π* transitions.

For analogues 1 (**A1**, **B1** and **C1**), the B-band appeared at ~400 nm while the Q-band appeared at ~560 nm. These results reveal that adding different substituent groups at *meso*-position of porphyrin core (analogues 1) do not change configuration in electronic transition, the absorption maxima were not significantly shifted, see **Figure 9a**. Furthermore, when adding a strong withdrawing group in analogues 2, the B-band were red shifted, which appeared at 412, 439 and 466 nm for **A2**, **B2** and **C2**, respectively, while the Q-band appears at ~600 nm, see **Figure 9b**. These results indicate that introducing electron-withdrawing groups to the acceptor part of porphyrin dyes can fine-tune the effective conjugation length of π-spacer and give rise to light harvesting efficiency.

3.5 Adsorption of dyes on the $(TiO_2)_{38}$ cluster

It is well known that the absorption spectrum of free dyes can be affected when adsorbed onto the TiO_2 surface due to the interaction between the dyes and the TiO_2. This interaction determines the electron injection efficiency in which the photo-excited electrons transfer from the dyes into the CB of TiO_2. To reveal the electronic structure involved in the dye/semiconductor charge transfer process between the dyes and the TiO_2 surface upon photoexcitation, we simulated the **A1** (with acetic acid as acceptor) and **A2** (with

cyanoacrylic acid as acceptor) adsorbed on $(TiO_2)_{38}$ surfaces representing the complex structure of dye $(TiO_2)_{38}$ to compare the effect of different electron acceptor groups on the adsorption property of the designed dyes. These two dyes share the same Zn-porphyrin and number of benzene unit in the π-spacer but have different anchoring group. The optimized structures of dye $(TiO_2)_{38}$ using DMol[3] are illustrated in **Figure 10**.

It is commonly known that the more favourable grafting configuration of the cyanoacrylic/acetic acid onto the TiO_2 surface is bidentate chemisorption.[53-55] So we only modelled the bidentate grafting adsorptions mode of **A1** and **A2** dyes onto the TiO_2 surface. Two Ti–O bonds from both **A1** and **A2** grafted onto $(TiO_2)_{38}$ clusters were found to be in the range of 2.05–2.17 Å. The dihedral angle between porphyrin ring and benzene ring (T1) of **A1** was calculated to be 75.20 degrees, when adding CN group in **A2** this T1 was decreased to 63.13 degrees resulting in stronger ICT and a potentially more efficient electron injection process on TiO_2 surface in **A2** dye. Consequently, the calculated adsorption energy (E_{ads}) of the **A2**-$(TiO_2)_{38}$ complex was computed to be 20.71 kcal/mol performing stronger interactions than that of 16.60 kcal/mol for **A1**-$(TiO_2)_{38}$, see **Table 4.** Furthermore, in order to investigate the mechanism of electron injection from dyes into TiO_2 surface we used the DFT/TD-DFT calculations as implemented in the Gaussian09 program. The excitation energies and the electronic transitions are summarized in **Table 5** and the frontier molecular orbitals of excited-state structures of dye-$(TiO_2)_{38}$ for **A1 and A2** are shown in **Figure 10**. We found two main transition for **A1** dye, the highest oscillator strength of 0.0425 was the linear combination of 0.43(H-1→L+62) - 0.49(H→L+58), the oscillator strength of 0.0104 was the linear combination of 0.51(H→L+58) + 0.43(H-1→L+58), both transition have been assigned to π-π* transition of a porphyrin ring. The HOMO-1 and HOMO level for **A1** showed the electron density located on π-bond of the porphyrin core, whereas the LOMO+62 and LUMO+58 levels for **A1** showed the electron density mainly located on π anti-bonding

of the porphyrin core. The electron injection process from **A1** to $(TiO_2)_{38}$ surface was rarely observed, see **Figure 11a**. On the other hand, electron injection process were detected in **A2**-$(TiO_2)_{38}$ complex which was 0.39(H→L+3) transition shown in **Figure 11b.** These results strongly indicate that the strong withdrawing group in the acceptor part of an **A2**-porphyrin dye plays a crucial role improving intramolecular charge transfer properties and induce an electron injection process form anchoring group of porphyrin dye to $(TiO_2)_{38}$ surface, which may improve the photo current as well as the conversion efficiency of the DSSCs cells.

Conclusion

We have designed our new dyes based on porphyrins ZnTCPP with typical porphyrin moieties as donors and the carboxyl-containing groups as acceptors (**A1**, **B1** and **C1**) to study the effect of different *meso*-substituted linkages. We found that our dyes, especially **C1** with thiophene linker, exhibited twisted conformation between the porphyrin macrocycle and *meso*-substituted linkages, which resulted in blocking of the conjugation of conjugated backbone. These results confirmed, by frontier molecular orbital plot, our calculations indicating that the charge-separated states take place slightly. To improve photo-induced intramolecular-charged transfer ability of the meso-linked zinc porphyrin sensitizer, which is the challenging problem for processing effectively injected electrons into the conduction band of TiO_2 in the DSC devices, a strong withdrawing group (CN) was introduced. The density difference plot for the first lowest excitation (ρ_{S1}-ρ_{S0}) of **A2**, **B2** and **C2** exhibited dramatically improved ICT properties. In addition, calculated excitation energies and UV/Vis absorption spectra were carried out by TD-DFT method, we found that adding different substituent groups at the *meso*-position of the porphyrin core (analogues 1), the absorption maxima were not significantly shifted whereas adding strong withdrawing group in analogues 2, the B-band were significantly red shifted which appeared at 412, 439 and 466 nm for **A2**, **B2** and **C2**. These results indicate that introducing electron-withdrawing groups to the

acceptor part of porphyrin dyes can fine-tune the effective conjugation length of π-spacer and give rise to efficient conversion of light to electricity. Moreover, the adsorption of these dyes on the TiO_2 anatase (101) surface and the electron injection mechanism were also investigated. The adsorption energy (E_{ads}) of **A1** and **A2** were calculated to be 16.60 and 20.71 kcal/mol, respectively, indicating the significantly stronger electronic coupling strengths of the anchoring group of **A2** and the TiO_2 surface. The electron injection process from the **A1** to $(TiO_2)_{38}$ surface was rarely observed while direct charge-transfer transition in the **A2**-$(TiO_2)_{38}$ interacting system was detected as a transition of HOMO to LOMO+3. These results strongly indicated that **A2** with strong withdrawing group in acceptor part of a porphyrin dye plays a crucial role improving intramolecular charge transfer properties and an induced electron injection process form anchoring group of a porphyrin dye to $(TiO_2)_{38}$ surface, which may improve the photo current as well as the conversion efficiency of the DSSCs cells. The successful study of these theoretical calculations may be used as the first attempt to tune the molecular orbital energy levels and improve the light absorption properties in a screening step, providing newly designed effective sensitizers in further experimental synthesis.

Acknowledgments

The authors would like to express grateful acknowledgement to the Department of Chemistry, Faculty of Science, Ubon Ratchathani University and Chiang Mai University. Financial support from the Center for Innovation in Chemistry (PERCH-CIC), Office of the Higher Education Commission, Ministry of Education, the National Science and Technology Development Agency [SPA A5: Solar Cell (10ISRA05)] is gratefully acknowledged. The Graduate School of Chiang Mai University and National Nanotechnology Center (NANOTEC) are also acknowledged.

References

1. B. O'Regan and M. Grätzel, *Nature*, 1991, **353**, 737-740.
2. M. Grätzel, *Journal of Photochemistry and Photobiology C: Photochemistry Reviews*, 2003, **4**, 145-153.
3. M. Grätzel, *Journal of Photochemistry and Photobiology A: Chemistry*, 2004, **164**, 3-14.
4. M. K. Nazeeruddin, A. Kay, I. Rodicio, R. Humphry-Baker, E. Mueller, P. Liska, N. Vlachopoulos and M. Grätzel, *Journal of the American Chemical Society*, 1993, **115**, 6382-6390.
5. P. Péchy, T. Renouard, S. M. Zakeeruddin, R. Humphry-Baker, P. Comte, P. Liska, L. Cevey, E. Costa, V. Shklover, L. Spiccia, G. B. Deacon, C. A. Bignozzi and M. Grätzel, *Journal of the American Chemical Society*, 2001, **123**, 1613-1624.
6. A. Yella, R. Humphry-Baker, B. F. E. Curchod, N. Ashari Astani, J. Teuscher, L. E. Polander, S. Mathew, J.-E. Moser, I. Tavernelli, U. Rothlisberger, M. Grätzel, M. K. Nazeeruddin and J. Frey, *Chemistry of Materials*, 2011, **25**, 2733-2739.
7. X.-H. Zhang, Y. Cui, R. Katoh, N. Koumura and K. Hara, *The Journal of Physical Chemistry C*, 2010, **114**, 18283-18290.
8. Q. Wang, W. M. Campbell, E. E. Bonfantani, K. W. Jolley, D. L. Officer, P. J. Walsh, K. Gordon, R. Humphry-Baker, M. K. Nazeeruddin and M. Grätzel, *The Journal of Physical Chemistry B*, 2005, **109**, 15397-15409.
9. W. M. Campbell, K. W. Jolley, P. Wagner, K. Wagner, P. J. Walsh, K. C. Gordon, L. Schmidt-Mende, M. K. Nazeeruddin, Q. Wang, M. Grätzel and D. L. Officer, *The Journal of Physical Chemistry C*, 2007, **111**, 11760-11762.
10. E. M. Barea, V. Gónzalez-Pedro, T. Ripollés-Sanchis, H.-P. Wu, L.-L. Li, C.-Y. Yeh, E. W.-G. Diau and J. Bisquert, *The Journal of Physical Chemistry C*, 2011, **115**, 10898-10902.
11. N. Xiang, X. Huang, X. Feng, Y. Liu, B. Zhao, L. Deng, P. Shen, J. Fei and S. Tan, *Dyes and Pigments*, 2011, **88**, 75-83.
12. M. P. Balanay and D. H. Kim, *Current Applied Physics*, 2011, **11**, 109-116.
13. A. Yella, H.-W. Lee, H. N. Tsao, C. Yi, A. K. Chandiran, M. K. Nazeeruddin, E. W.-G. Diau, C.-Y. Yeh, S. M. Zakeeruddin and M. Grätzel, *Science* 2011, **334**, 629-634.
14. M. P. Balanay and D. H. Kim, *Journal of Molecular Structure: THEOCHEM*, 2009, **910**, 20-26.
15. M. Gouterman, *The Journal of Chemical Physics*, 1959, **30**, 1139-1161.
16. L. Cai, T. Moehl, S.-J. Moon, J.-D. Decoppet, R. Humphry-Baker, Z. Xue, L. Bin, S. M. Zakeeruddin and M. Grätzel, *Organic Letters*, 2014, **16**, 106-109.
17. S. Chaurasia, C.-Y. Hsu, H.-H. Chou and J. T. Lin, *Organic Electronics*, 2014, **15**, 378-390.
18. K. Lim, C. Kim, J. Song, T. Yu, W. Lim, K. Song, P. Wang, N. Zu and J. Ko, *The Journal of Physical Chemistry C*, 2011, **115**, 22640-22646.
19. L. Pelleja , C. V. Kumar, J. N. Clifford and E. Palomares, *The Journal of Physical Chemistry C*, 2014, (accepted manuscript).
20. C. Wang, Y. Fang, Z. Cao, H. Huang, B. Zhao, H. Li, Y. Liu and S. Tan, *Dyes and Pigments*, 2013, **97**, 405-411.
21. J. Zhang, H.-B. Li, Y. Geng, S.-Z. Wen, R.-L. Zhong, Y. Wu, Q. Fu and Z.-M. Su, *Dyes and Pigments*, 2013, **99**, 127-135.
22. M. Cheng, X. Yang, F. Zhang, J. Zhao and L. Sun, *The Journal of Physical Chemistry C*, 2013, **117**, 9076-9083.
23. J. Feng, Y. Jiao, W. Ma, M. K. Nazeeruddin, M. Grätzel and S. Meng, *The Journal of Physical Chemistry C*, 2013, **117**, 3772-3778.
24. C.-R. Zhang, L. Liu, Z.-J. Liu, Y.-L. Shen, Y.-T. Sun, Y.-Z. Wu, Y.-H. Chen, L.-H. Yuan, W. Wang and H.-S. Chen, *Journal of Molecular Graphics and Modelling*, 2012, **38**, 419-429.
25. P. J. Walsh, K. C. Gordon, D. L. Officer and W. M. Campbell, *Journal of Molecular Structure: THEOCHEM*, 2006, **759**, 17-24.

26. R. Ma, P. Guo, H. Cui, X. Zhang, M. K. Nazeeruddin and M. Graฬtzel, *The Journal of Physical Chemistry A*, 2009, **113**, 10119-10124.
27. M. P. Balanay, K. H. Kim, S. H. Lee and D. H. Kim, *Journal of Photochemistry and Photobiology A: Chemistry*, 2012, **248**, 63-72.
28. Y. Tachibana, S. A. Haque, I. P. Mercer, J. R. Durrant and D. R. Klug, *The Journal of Physical Chemistry B*, 2000, **104**, 1198-1205.
29. J. K. Park, H. R. Lee, J. Chen, H. Shinokubo, A. Osuka and D. Kim, *The Journal of Physical Chemistry C*, 2008, **112**, 16691-16699.
30. Q. Wang, W. M. Campbell, E. E. Bonfantani, K. W. Jolley, D. L. Officer, P. J. Walsh, K. Gordon, R. Humphry-Baker, M. K. Nazeeruddin and M. Grรคtzel, *The Journal of Physical Chemistry B*, 2005, **109**, 15397-15409.
31. C.-W. Lee, H.-P. Lu, C.-M. Lan, Y.-L. Huang, Y.-R. Liang, W.-N. Yen, Y.-C. Liu, Y.-S. Lin, E. W.-G. Diau and C.-Y. Yeh, *Chemistry – A European Journal*, 2009, **15**, 1403-1412.
32. H.-P. Lu, C.-L. Mai, C.-Y. Tsia, S.-J. Hsu, C.-P. Hsieh, C.-L. Chiu, C.-Y. Yeh and E. W.-G. Diau, *Physical Chemistry Chemical Physics*, 2009, **11**, 10270-10274.
33. T. Kaewin, K. Sirithip, P. Thongkasee, T. Sudyoadsuk, S. Namuangruk, S. Jungsuttiwong and V. Promarak, in *Dye-Sensitized Solar Cells*, Ubon Ratchathani, Editon edn., 2014.
34. A. D. Becke, *The Journal of Chemical Physics*, 1993, **98**, 5648-5652.
35. B. Miehlich, A. Savin, H. Stoll and H. Preuss, *Chemical Physics Letters*, 1989, **157**, 200-206.
36. C. Lee, W. Yang and R. G. Parr, *Physical Review B*, 1988, **37**, 785.
37. N. N. Matsuzawa, A. Ishitani, D. A. Dixon and T. Uda, *The Journal of Physical Chemistry A*, 2001, **105**, 4953-4962.
38. Y. Takano and K. N. Houk, *Journal of Chemical Theory and Computation*, 2004, **1**, 70-77.
39. M. J. Frisch, G. W. Trucks, H. B. Schlegel, G. E. Scuseria, M. A. Robb, J. R. Cheeseman, G. Scalmani, V. Barone, B. Mennucci, G. A. Petersson, H. Nakatsuji, M. Caricato, X. Li, H. P. Hratchian, A. F. Izmaylov, J. Bloino, G. Zheng, J. L. Sonnenberg, M. Hada, M. Ehara, K. Toyota, R. Fukuda, J. Hasegawa, M. Ishida, T. Nakajima, Y. Honda, O. Kitao, H. Nakai, T. Vreven, J. A. Montgomery, Jr., J. E. Peralta, F. Ogliaro, M. Bearpark, J. J. Heyd, E. Brothers, K. N. Kudin, V. N. Staroverov, R. Kobayashi, J. Normand, K. Raghavachari, A. Rendell, J. C. Burant, S. S. Iyengar, J. Tomasi, M. Cossi, N. Rega, J. M. Millam, M. Klene, J. E. Knox, J. B. Cross, V. Bakken, C. Adamo, J. Jaramillo, R. Gomperts, R. E. Stratmann, O. Yazyev, A. J. Austin, R. Cammi, C. Pomelli, J. W. Ochterski, R. L. Martin, K. Morokuma, V. G. Zakrzewski, G. A. Voth, P. Salvador, J. J. Dannenberg, S. Dapprich, A. D. Daniels, O. Farkas, J. B. Foresman, J. V. Ortiz, J. Cioslowski and D. J. Fox, **Gaussian 09, Revision C.01, Gaussian, Inc., Wallingford CT, 2009.**
40. S. I. Gorelsky and A. B. P. Lever, *Journal of Organometallic Chemistry*, 2001, **635**, 187-196.
41. M. O. b. Noel, L. T. Adam and M. L. Karol, *Journal of Computational Chemistry*, 2008, **29**, 839-845.
42. B. Delley, *Journal of Chemical Physics* 1990, **92**, 508-517.
43. B. Delley, *Physical Review B*, 2002, **66**, 1-9.
44. T. Yakhanthip, S. Jungsuttiwong, S. Namuangruk, N. Kungwan, V. Promarak, T. Sudyoadsuk and P. Kochpradist, *Journal of Computational Chemistry*, 2011, **32**, 1568-1576.
45. J. P. Perdew, K. Burke and M. Ernzerhof, *Physical Review Letters*, 1996, **77**, 3865.
46. R. Ma, P. Guo, L. Yang, L. Guo, X. Zhang, M. K. Nazeeruddin and M. Grätzel, *The Journal of Physical Chemistry A*, 2010, **114**, 1973-1979.
47. T. Yakhanthip, S. Jungsuttiwong, S. Namuangruk, N. Kungwan, V. Promarak, T. Sudyoadsuk and P. Kochpradist, *Journal of Computational Chemistry*, 2011, **32**, 1568-1576.
48. Y.-X. Weng, Y.-Q. Wang, J. B. Asbury, H. N. Ghosh and T. Lian, *The Journal of Physical Chemistry B*, 1999, **104**, 93-104.
49. M. Yang, D. W. Thompson and G. J. Meyer, *Inorganic Chemistry*, 2000, **39**, 3738-3739.
50. M. Khoudiakov, A. R. Parise and B. S. Brunschwig, *Journal of the American Chemical Society*, 2003, **125**, 4637-4642.

51. X. Chen and S. S. Mao, *Chemical Reviews*, 2007, **107**, 2891-2959.
52. M. Gouterman, *Journal of Molecular Spectroscopy*, 1961, **6**, 138-163.
53. K. Hara, T. Sato, R. Katoh, A. Furube, Y. Ohga, A. Shinpo, S. Suga, K. Sayama, H. Sugihara and H. Arakawa, *The Journal of Physical Chemistry B*, 2002, **107**, 597-606.
54. S. Namuangruk, R. Fukuda, M. Ehara, J. Meeprasert, T. Khanasa, S. Morada, T. Kaewin, S. Jungsuttiwong, T. Sudyoadsuk and V. Promarak, *The Journal of Physical Chemistry C*, 2012, **116**, 25653-25663.
55. M. K. Nazeeruddin, R. Humphry-Baker, P. Liska and M. Grätzel, *The Journal of Physical Chemistry B*, 2003, **107**, 8981-8987.